Detection and mapping of seagrass meadows at Ritchie's archipelago using Sentinel 2A satellite imagery

Sharad Bayyana[1,*], Satish Pawar[1], Swapnali Gole[2], Sohini Dudhat[2], Anant Pande[2], Debashis Mitra[3], Jeyaraj Antony Johnson[4] and Kuppusamy Sivakumar[2]

[1]Indian Institute of Remote Sensing, Dehradun 248 001, India
[2]Department of Endangered Species Management, Wildlife Institute of India, Dehradun 248 002, India
[3]Marine and Atmospheric Science Department, Indian Institute of Remote Sensing, Dehradun 248 001, India
[4]Department of Habitat Ecology, Wildlife Institute of India, Dehradun 248 002, India

This study presents an attempt to utilize seagrass data acquired from field surveys to compare classification models for mapping seagrasses using Sentinel-2A satellite data. Out of three models tested, viz. Random Forest, Support Vector Machine and K-Nearest Neighbor; Random Forest classification model proved most effective in the given scenario with 0.99 model accuracy. Seagrasses present as deep as 21 m were detected post water column correction, presenting the capability of Sentinel-2A satellite in detecting submerged benthic habitat.

Keywords: Depth Invariant Index, Ritchie's archipelago, seagrass, Sentinel-2A.

SEAGRASS meadows, one of the most productive ecosystems on the planet, are estimated to lose 7% of their global area annually[1]. Spatial data analysis for seagrass studies towards their sustainable management and conservation has been an emerging field. Globally, satellite remote sensing tools have proven to be cost effective in comparison to conventional field surveys[2–8] and traditional geospatial methods such as aerial photography[9]. Since, satellite sensors are repeatable in their path and are geometrically accurate, change detection in seagrass distribution over temporal scale is possible[10–12]. Landsat imagery has been efficiently used in seagrass and benthic substrate mapping, despite its spectral and spatial limitations[12–15]. Multispectral imagery from compact airborne spectrographic imager (CASI) with satellite imagery of Landsat and Spot, has been shown to exhibit more accurate results from airborne high-resolution sensor compared to aerial photography in classification of submerged benthic features including seagrasses[2].

Sensing of submerged benthic vegetation in the coastal waters is achieved with multispectral observations (400–650 nm) of reflected radiance in the visible range which is enhanced with finer spatial resolution[16]. Certain regression models developed for mapping benthic features have opened up the doors to overcome the limitations of attenuation of radiance within the water column[17–19]. Assuming that variance in reflectance from same benthic substrate is primarily due to its presence at various depths and the diffused attenuation coefficient (K_d) is same for all the bands[17,18], regression from logarithmic values of individual bands provides proxy attenuation coefficients which are independent of depth[20]. Assessment of submerged sea grasses is reliable with remote sensing when appropriate correction (such as water depth correction) is applied to satellite images[21]. Medium resolution multispectral satellite images from Landsat OLI were effective in mapping of submerged benthic features with application of depth invariant index (DII), which is independent of depth effect[22]. High resolution multispectral imagery such as Sentinel-2A with 10 m spatial resolution has also proved effective to detect and estimate the cover of seagrass beds along the coast of Lombok in Indonesia[23]. The quality of results post DII when utilized for VHR Worldview-2 imageries was significantly high (up to 83% at Kotok Island in Indonesia)[24].

In India, seagrass are distributed along the coastline of nine states and two union territories with major patches found along Tamil Nadu (Palk Bay and Gulf of Mannar), Odisha, Gujarat, Lakshadweep Islands and Andaman and Nicobar Islands[25]. Remote sensing for the seagrass detection was first initiated at Lakshadweep islands to study the coral reefs and seagrass beds using black and white aerial photographs[26]. Later, loss of seagrass habitats in Gulf of Mannar group of islands due to anthropogenic activities was detected using LISS III satellite imagery[27]. Seagrass area was estimated to be around 85.5 sq. km around the islands of Gulf of Mannar based on IRS-1D LISS III satellite data from 1998 (ref. 28).

Earlier, a few studies have utilized conventional field survey methods to map seagrass ecosystems in the Andaman and Nicobar group of islands[29–31]. One study used satellite geospatial data (LISS III and LISS IV) for the mapping across the entire Andaman islands[32]. Seagrass meadows in Andaman and Nicobar Islands serve as foraging grounds for globally threatened species such as dugongs, green sea turtles[33], and act as nurseries for several species of fish and invertebrates and thus support fisheries in the islands. In the light of proposed infrastructure developments in the islands[34], understanding the extent of seagrass distribution in the islands will be useful in identifying critical areas to aid their conservation and management.

In this study, we mapped the seagrass meadows at Ritchie's archipelago (henceforth RA; 11°46′N–12°19′N and 92°54′E–93°08′E) within the Andaman and Nicobar group of islands using multi-spectral imager (MSI) Sentinel-2A satellite imagery (Supplementary Table 1). Ritchie's archipelago is a group of 13 islands, east of the main group of Andaman islands, consisting of two

*For correspondence. (e-mail: bsharad0404@gmail.com)

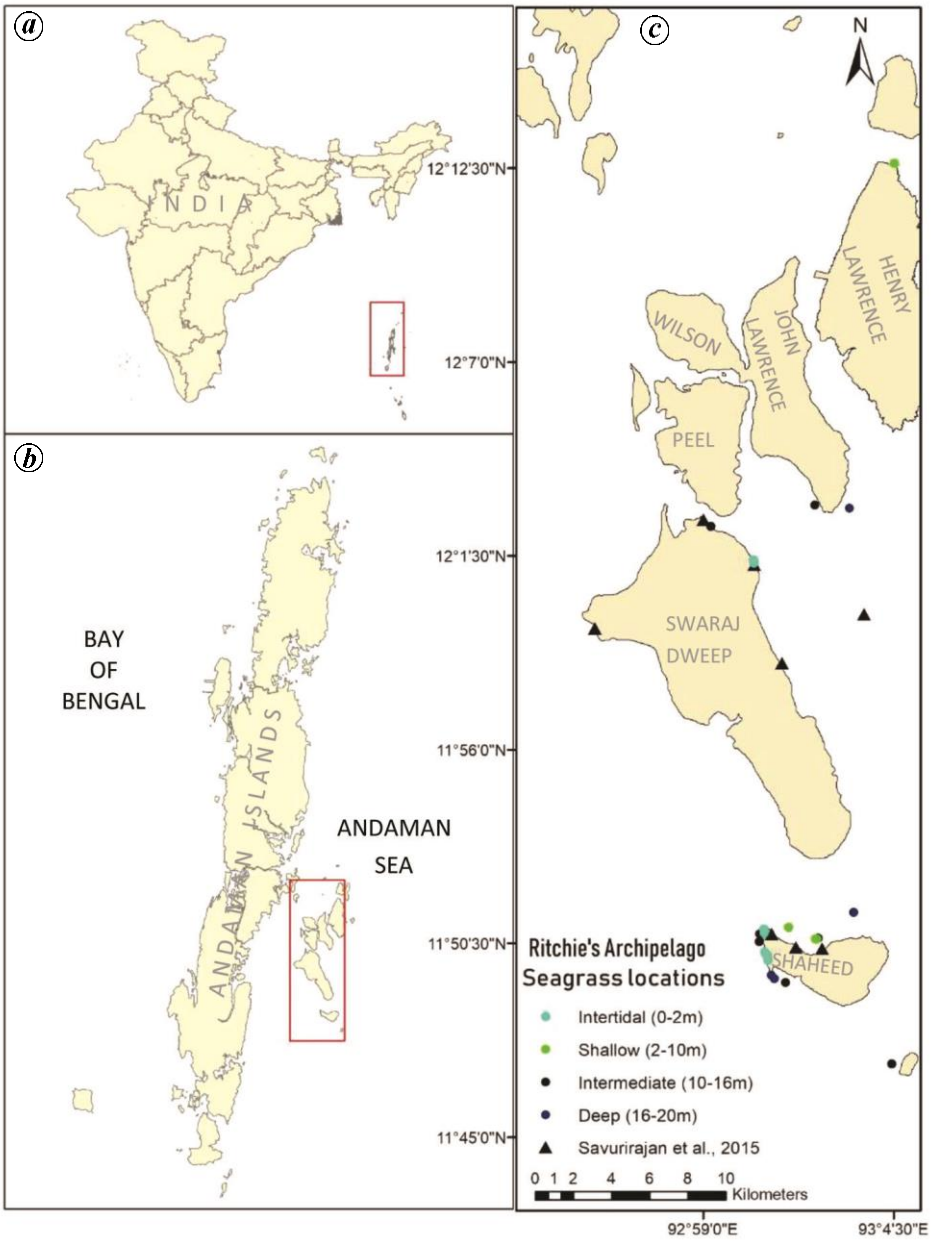

Figure 1. Study area map of Ritchie' Archipelago, Andaman and Nicobar Islands with seagrass locations.

inhabited (Havelock, now *Swaraj Dweep* and; Neil, now *Shaheed Dweep*) and 11 uninhabited islands (North button, middle button, south button, Outram, Inglis, Henry Lawrence, John Lawrence, Wilson, Nicholson, Peel and Sir Hugh Ross) spread across an area of 225 sq. km (ref. 35) (Figure 1). Seven of these islands, viz. North button, middle button, south button, Outram, Inglis, Henry Lawrence and John Lawrence, form part of the Rani Jhansi Marine National Park protected area whereas Sir Hugh Ross is a Wildlife Sanctuary. With a tidal amplitude of 3 m during spring and neap tide, semidiurnal tide is seen in the region.

We carried out seagrass surveys using line intercept transects (LITs; Figure 2) at intertidal and sub tidal areas at various depths at RA in the month of March and April 2018 (Supplementary Table 2). Subtidal areas were characterized using SCUBA diving whereas the intertidal areas were surveyed on-foot. Line intercept transects (50 m long; LIT) were deployed perpendicular to the shore to assess meadow characteristics (McKenzie and Yoshida 2012). At each transect, seagrass cover, species composition, algal cover and substrate type were recorded using a 50 × 50 cm quadrate (Supplementary Figure 1) along with GPS location (Garmin etrex 30) and depth (Aqualung i300 dive computer) for generating training sets for supervised classification and for training data accuracy assessment of the prediction models. In addition

Table 1. Depth-wise segregation of seagrass locations at Ritchie's Archipelago, Andaman and Nicobar Islands

Island	Transect points	Seagrass class	Depth range
Shaheed Dweep	NB1, NB2, NB3, NB4 LX1, LX2	Intertidal	0–2 m
Swaraj Dweep	DL1, DL2		
Shaheed Dweep	AQ, BH2, BH3	Shallow	2–10 m
Henry Lawrence	HL		
Shaheed Dweep	NU1, NU2, NU3, MG3, BH1	Intermediate	10–16 m
Swaraj Dweep	NR		
Hugh Ross	CHN		
John Lawrence	JL2		
Shaheed Dweep	MG1, MG2, BB,	Deep	16–20 m
John Lawrence	JL1		

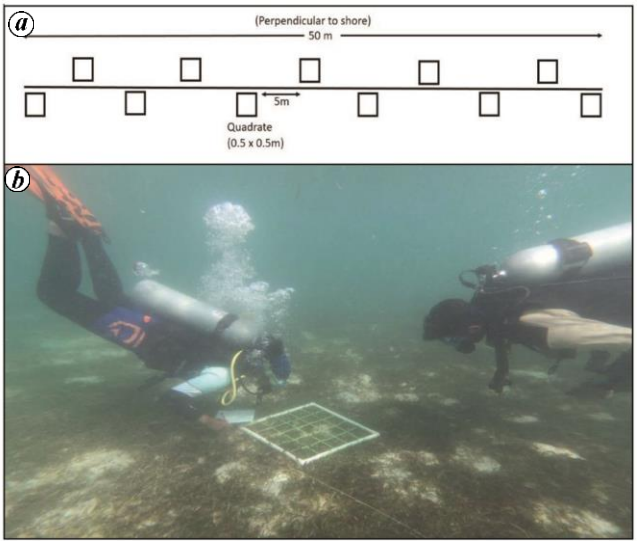

Figure 2. ***a***, Illustration of Line Intercept Transect survey method. ***b***, Image showing quadrant survey along the transect line.

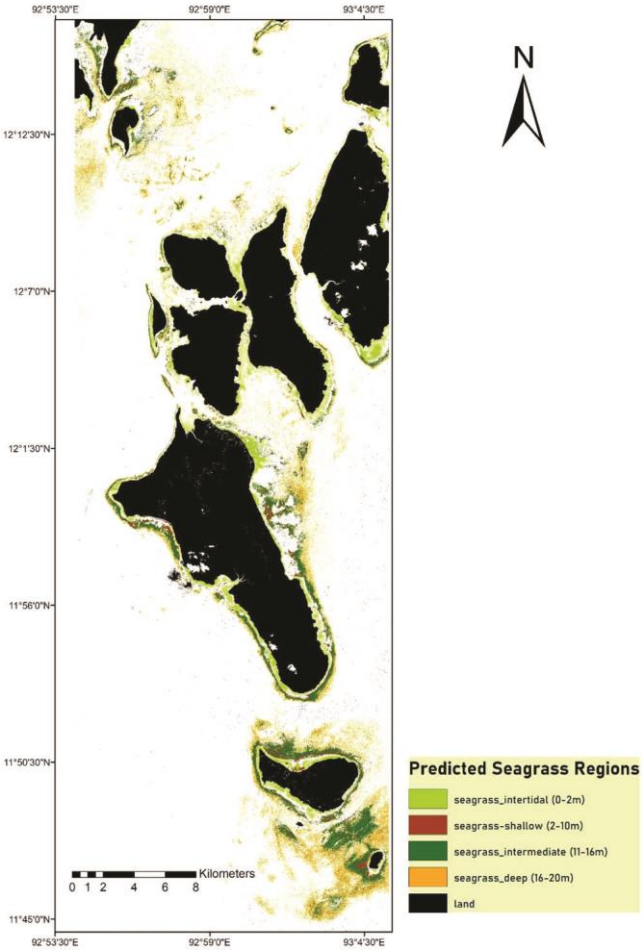

Figure 3. Random Forest Classification Map of Ritchie's archipelago from Sentinel 2A image. Image was acquired on 22 March 2018 at approximately 10 : 30 local time (satellite over-pass time). Tidal range on the particular day was 0.28–2.06 m.

to this, we used seagrass locations provided for RA from Savurirajan *et al.*[31], to cross-validate the efficiency of the prediction models.

We accessed the Sentinel-2A level 1C (top of atmosphere radiance) imagery acquired on 22 March 2018 (10 : 30 local time overpass) over the South Andaman region by European Space Agency (ESA) (http://scihub.copernicus.eu). The tidal range on the date of acquisition was 0.28–2.06 m. Atmospheric correction was done to 'top of surface, water leaving reflectance' product using 'sen2cor' additional plug-in[36] on SNAP 6.0 platform by ESA (https://step.esa.int/main/download/snap-download/) for Sentinel series image processing. Visible bands (band 2-blue, 3-green and 4-red) of 10 m spatial resolution were utilized considering their capability to penetrate water up to considerable depth[16]. We used the Lyzenga method[18] to obtain coefficient values to generate a normalized index value independent of the depth factor. Reflectance values from each band were extracted using 'point sampling tool' plug-in in QGIS. Simple linear regression was carried out using the logarithmic values of reflectance between two bands. The coefficient of the slopes of regression were utilized as attenuation coefficient. Three bands generated from original band combination (i.e. band blue–green, green–red and red–blue) were stacked to produce an RGB layer of depth invariant index.

We carried out supervised classification to derive four depth-based classes for seagrass locations obtained from

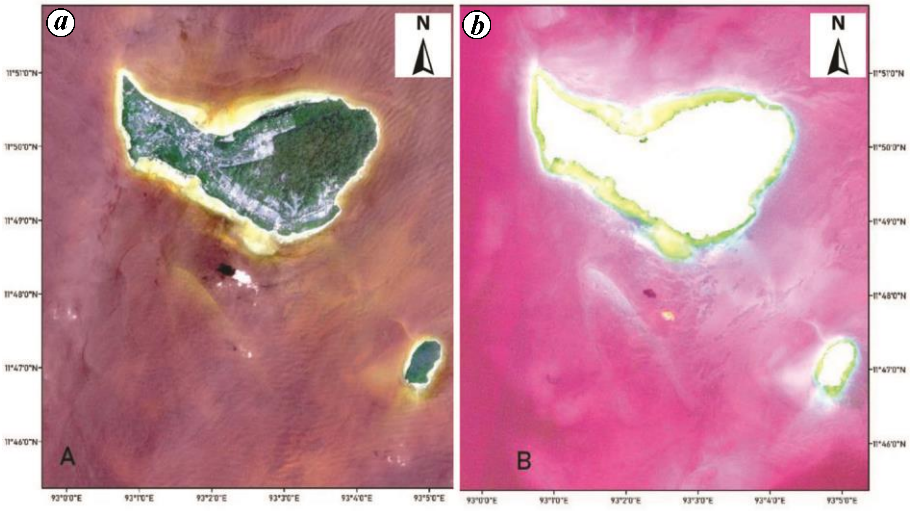

Figure 4. ***a***, True colour composite of subset of *Shaheed Dweep* Island from Sentinel-2A image. ***b***, RGB stack of depth invariant Index of bands of same image.

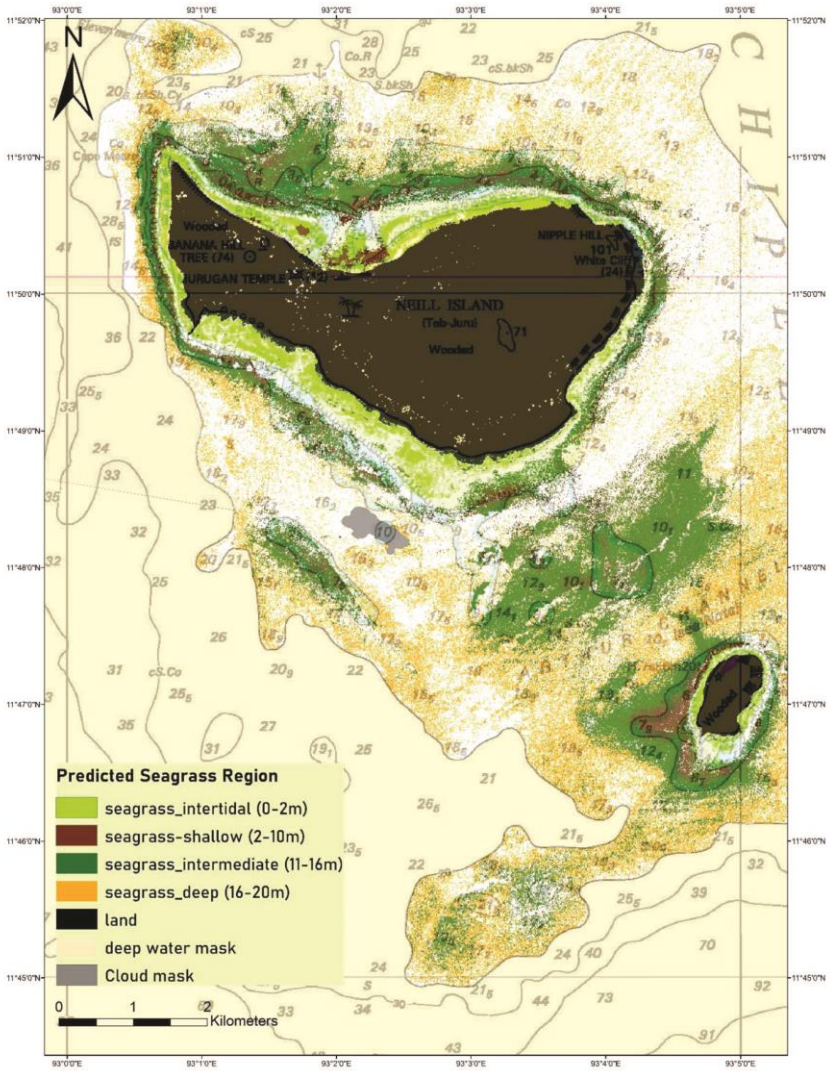

Figure 5. Classified map of *Shaheed Dweep* Island from Sentinel-2A image using Random Forest model.

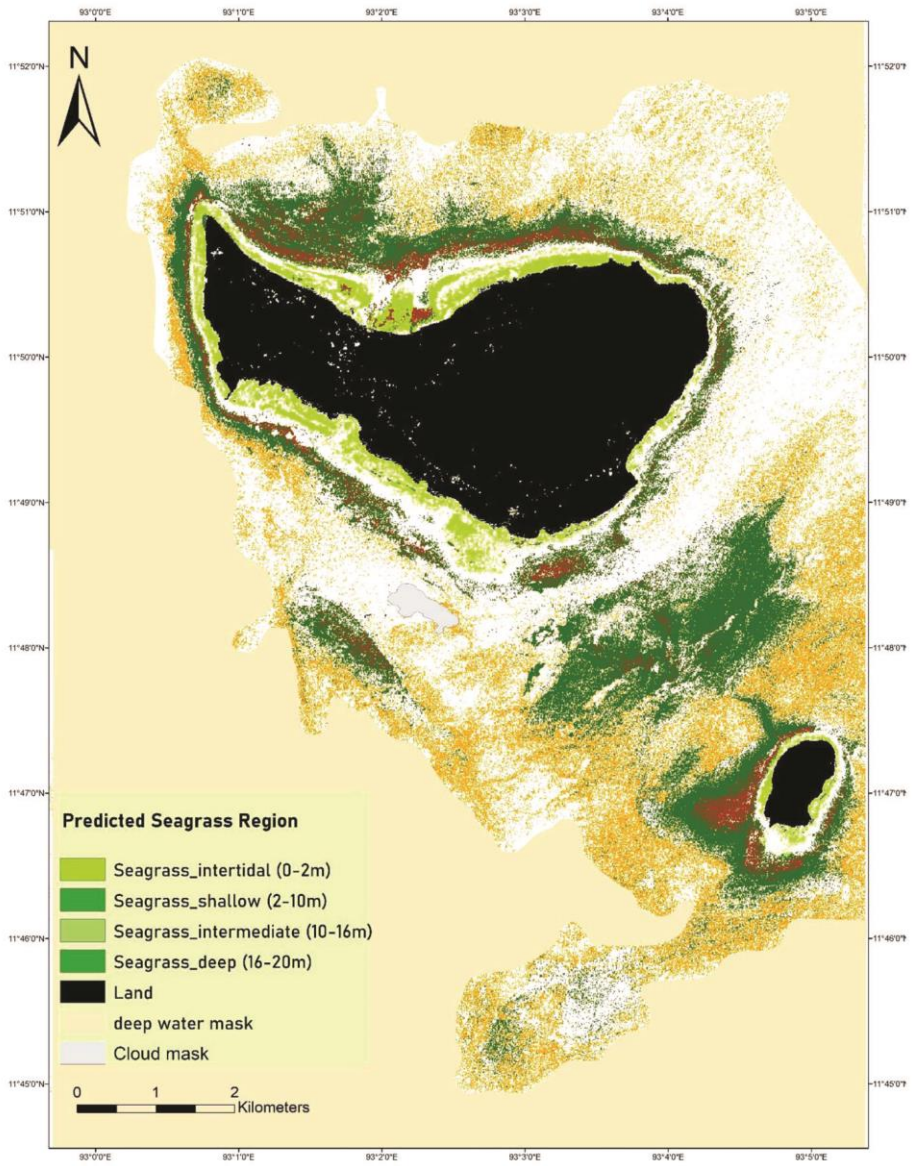

Figure 6. Classified map of *Shaheed Dweep* Island from Sentinel-2A image using K-Nearest Neighbor model.

Table 2. Training data accuracy of respective models used for supervised classification of Sentinel 2A images

Classification models	Overall accuracy	Kappa accuracy
Random forest	0.99	0.97
Support vector machine	0.96	0.93
K-nearest neighbor	0.96	0.93

field surveys (intertidal: 0–2 m; shallow: 2–10 m, intermediate: 10–16 m and; deep: 16–20 m) and validated with NHO bathymetry chart (Chart 4016, NHO; see Table 1). We used 70% of the seagrass locations obtained from field surveys to generate Region of Interests (RoIs) to train three different models (Random Forest (RF), Support Vector Machine (SVM) and K-Nearest Neighbor (KNN)) on Program-R (https://www.R-project.org/) using remaining 30% field data for model validation. For the cross validation of the classification models, transect NB3 LX2 for Intertidal, AQ for Shallow, CHN NU2 for Intermediate class and MG1 for Deep class were utilized. Classification models were run on R-studio IDE platform using 'caret', 'rgdal', 'raster', 'e1071' and 'tidyverse' packages. Further validation was done using previously published seagrass locations[31] for *Swaraj Dweep* and *Shaheed Dweep* islands. Later, classified outputs were presented for *Shaheed Dweep* to clearly illustrate segregation of depth classes obtained from each model.

During field surveys, we recorded seagrasses at 24 locations within the RA, namely at Henry Lawrence

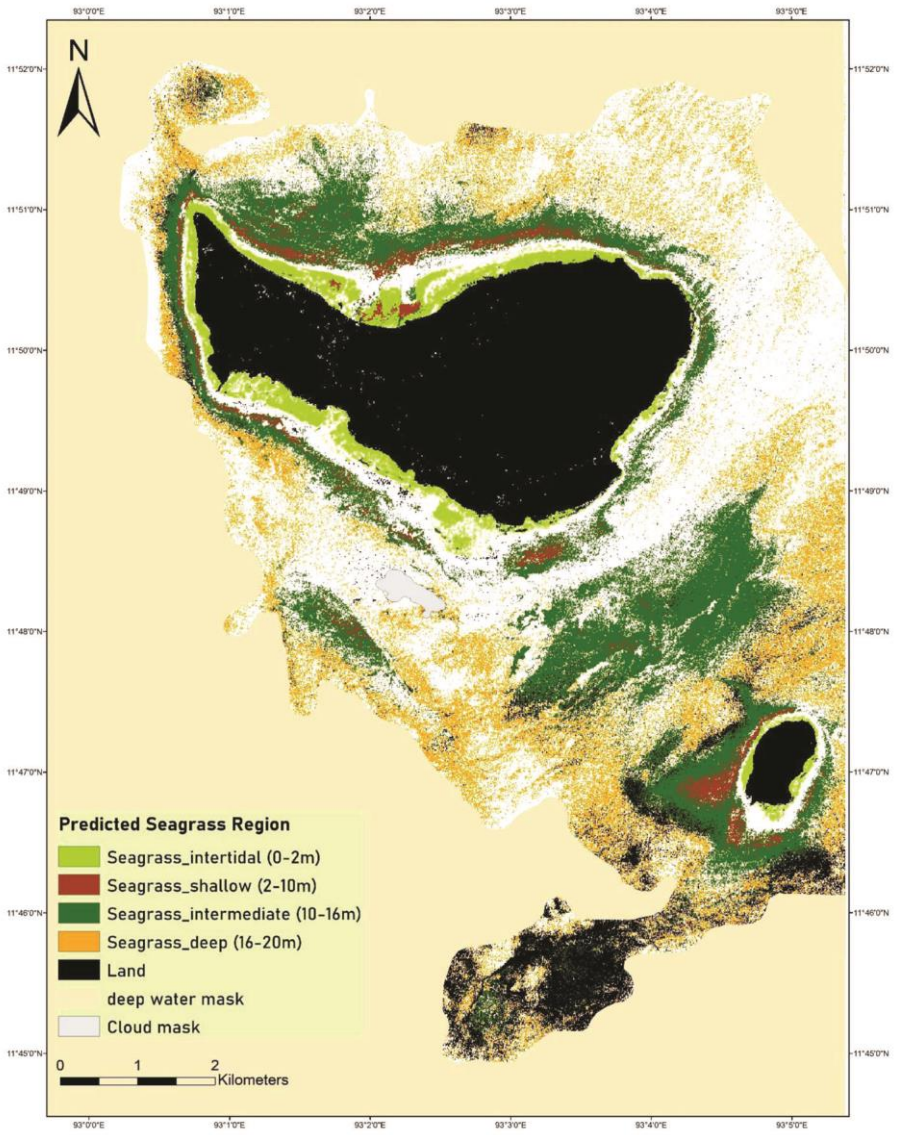

Figure 7. Classified map of *Shaheed Dweep* Island from Sentinel-2A image using Support Vector Machine model.

($n = 1$), John Lawrence ($n = 2$), *Swaraj Dweep* ($n = 3$), *Shaheed Dweep* ($n = 17$) and Sir Hugh Ross ($n = 1$) islands.

RF model (Figure 3) produced highest training data accuracy (0.99) for detecting seagrass in the study area followed by SVM and KNN (0.96) (Table 2). We obtained better signatures for the benthic features (Figure 4) using the water column correction method resulting in better classification. Seagrasses were detected at the depth of 20 m around *Shaheed Dweep* Island, complementing the field observations (Figure 5). Random Forest model (Figure 5) and K-Nearest Neighbor model (Figure 6) were able to detect all depth classes whereas SVM model was unable to detect the 'Deep – 16 to 20 m' class in addition to misclassification of land over the sea (Figure 7). All the models used in the study detected seagrasses in deep water (>25 m) which were ignored considering the limitations of Lyzenga Method[18] to detect seagrass beyond 25 m. The results show 50% accuracy using the data points obtained from Savurirajan *et al.*[31].

The sea around Andaman and Nicobar Islands are oligotrophic waters due to less nutrient availability[37]. This results in low turbidity and hence deeper penetration of sunlight which allows seagrasses to grow at deeper regions. In our study, there is a high possibility of mixed signals, as seagrass distribution in the Andaman Islands is known to be sparse and interspersed with sandy patches[32,33]. Moreover, the accuracy of the models might be affected due to seasonal shifting of seagrass with respect to the sand dunes and thus their locations might change from previously reported studies[38,31]. In comparison

to previously used LISS III and IV data[4,28,32], Sentinel-2A was efficient in seagrass detection at higher depths. Previous studies were restricted to a depth of 5 m only[22,32].

Our results establish the efficacy of Sentinel 2A satellite imagery for seagrass mapping at higher spatial scale as well as for deeper coastal waters. Supervised classification using RF model method proved to be better model for seagrass classification in the given scenario with limited field data (Supplementary Figure 2). Depth variant index improved the classification of underwater features for Sentinel-2A imagery. Seagrass detection was successful at the ground points used for the cross validation of the classification even for the deepest locations mapped in the study area (~21 m).

Despite mounting anthropogenic pressure on seagrass ecosystems and its associated species across the world[39,40], there is limited data on seagrass ecosystems in India[41,25]. With acceleration in human activities in the islands[34], threats such as coastal pollution including oil and plastic waste, mechanical damage from vessel anchors, higher turbidity from vessel movement and port construction activities, etc. are likely to intensify in the near future. Spatial mapping of seagrass beds in the islands using high resolution satellite imagery will be helpful in delineating critical areas for long-term change monitoring at a larger spatial scale.

1. Unsworth, R. K. and Cullen, L. C., Recognising the necessity for Indo-Pacific seagrass conservation. *Conserv. Lett.*, 2010, **3**(2), 63–73.
2. Mumby, P. J., Green, E. P., Edwards, A. J. and Clark, C. D., Measurement of seagrass standing crop using satellite and digital airborne remote sensing. *Mar. Ecol. Prog. Ser.*, 1997, **159**, 51–60.
3. Pasqualini, V., Pergent-Martini, C., Pergent, G., Agreil, M., Skoufas, G., Sourbes, L. and Tsirika, A., Use of SPOT 5 for mapping seagrasses: an application to *Posidonia oceanica*. *Remote Sens. Environ.*, 2005, **94**(1), 39–45.
4. Nobi, E. P. and Thangaradjou, T., Evaluation of the spatial changes in seagrass cover in the lagoons of Lakshadweep islands, India, using IRS LISS III satellite images. *Geocarto Int.*, 2012, **27**(8), 647–660.
5. Jensen, J. R., Inland wetland change detection in the Everglades Water Conservation Area 2A using a time series of normalized remotely sensed data. *Photogramm. Eng. Remote Sensing*, 1995, **61**(2), 199–209.
6. Clark, C. D., Ripley, H. T., Green, E. P., Edwards, A. J. and Mumby, P. J., Cover mapping and measurement of tropical coastal environments with hyperspectral and high spatial resolution data. *Int. J. Remote Sens.*, 1997, **18**(2), 237–242.
7. Malthus, T. J. and George, D. G., Airborne remote sensing of macrophytes in Cefni Reservoir, Anglesey, UK. *Aquat. Bot.*, 1997, **58**(3–4), 317–332.
8. Alberotanza, L., Hyperspectral aerial images. A valuable tool for submerged vegetation recognition in the Orbetello Lagoons, Italy. *Int. J. Remote Sens.*, 1999, **20**(3), 523–533.
9. Dekker, A., Brando, V., Anstee, J., Fyfe, S., Malthus, T. and Karpouzli, E., Remote sensing of seagrass ecosystems: use of spaceborne and airborne sensors. In *Seagrasses: Biology, Ecologyand Conservation*, Springer, Dordrecht, 2007, pp. 347–359.
10. Ward, D. H., Markon, C. J. and Douglas, D. C., Distribution and stability of eelgrass beds at Izembek Lagoon, Alaska. *Aquat. Bot.*, 1997, **58**(3–4), 229–240.
11. Macleod, R. D. and Congalton, R. G., A quantitative comparison of change-detection algorithms for monitoring eelgrass from remotely sensed data. *Photogramm. Eng. Remote Sensing*, 1998, **64**(3), 207–216.
12. Anstee, J. M., Dekker, A. G. and Brando, V. E., Retrospective change detection in a shallow coastal tidal lake: mapping seagrasses in Wallis Lake, Australia. In *Analysis of Multi-Temporal Remote Sensing Images*, 2004, pp. 277–285.
13. Chauvaud, S., Bouchon, C. and Maniere, R., Remote sensing techniques adapted to high resolution mapping of tropical coastal marine ecosystems (coral reefs, seagrass beds and mangrove). *Int. J. Remote Sensing*, 1998, **19**(18), 3625–3639.
14. Schweizer, D., Armstrong, R. A. and Posada, J., Remote sensing characterization of benthic habitats and submerged vegetation biomass in Los Roques Archipelago National Park, Venezuela. *Int. J. Remote Sensing*, 2005, **26**(12), 2657–2667.
15. Alkhatlan, A., Bannari, A., El-Battay, A., Al-Dawood, T. and Abahussain, A., Potential of Landsat-oli for seagrass and algae species detection and discrimination in Bahrain national water using spectral reflectance. In *IGARSS 2018–2018 IEEE International Geoscience and Remote Sensing Symposium*, Valencia, Spain, 2018, pp. 4043–4046.
16. Horning, N., Robinson, J. A., Sterling, E. J., Turner, W. and Spector, S., *Remote Sensing for Ecology and Conservation: A Handbook of Techniques*, Oxford University Press, 2010.
17. Lyzenga, D. R., Passive remote sensing techniques for mapping water depth and bottom features. *Appl. Opt.*, 1978, **17**(3), 379–383.
18. Lyzenga, D. R., Remote sensing of bottom reflectance and water attenuation parameters in shallow water using aircraft and Landsat data. *Int. J. Remote Sensing*, 1981, **2**(1), 71–82.
19. Sagawa, T., Boisnier, E., Komatsu, T., Mustapha, K. B., Hattour, A., Kosaka, N. and Miyazaki, S., Using bottom surface reflectance to map coastal marine areas: a new application method for Lyzenga's model. *Int. J. Remote Sensing*, 2010, **31**(12), 3051–3064.
20. Zoffoli, M., Frouin, R. and Kampel, M., Water column correction for coral reef studies by remote sensing. *Sensors*, 2014, **14**(9), 16881–16931.
21. Pu, R., Bell, S., Meyer, C., Baggett, L. and Zhao, Y., Mapping and assessing seagrass along the western coast of Florida using Landsat TM and EO-1 ALI/hyperion imagery. *Estuar., Coastal Shelf Sci.*, 2012, **115**, 234–245.
22. Geevarghese, G. A., Akhil, B., Magesh, G., Krishnan, P., Purvaja, R. and Ramesh, R., A comprehensive geospatial assessment of seagrass distribution in India. *Ocean Coast. Manage.*, 2018, **159**, 16–25.
23. Fauzan, M. A., Kumara, I. S., Yogyantoro, R., Suwardana, S., Fadhilah, N., Nurmalasari, I. and Wicaksono, P., Assessing the capability of Sentinel-2A data for mapping seagrass percent cover in Jerowaru, East Lombok. *Indonesian J. Geogr.*, 2017, **49**(2), 195–203.
24. Manuputty, A., Lumban-Gaol, J. and Agus, S. B., Seagrass mapping based on satellite image Worldview-2 by using depth invariant index method. *Indonesian J. Mar. Sci./Ilmu Kelautan*, 2016, **21**(1), 37–44.
25. Thangaradjou, T. and Bhatt, J. R., Status of seagrass ecosystems in India. *Ocean Coast. Manage.*, 2018, **159**, 7–15.
26. Jagtap, T. G. and Inamdar, S. N., Mapping of seagrass meadows from the Lakshadweep Islands (India), using aerial photographs. *J. Indian Soc. Remote Sens.*, 1991, **19**(2), 77–82.
27. Senthil Kumar, T. T. R. S. S. and Kannan, S., Seagrass resource assessment in the Mandapam coast of the Gulf of Mannar Biosphere Reserve, India. *Appl. Ecol. Environ. Res.*, 2008, **6**(1), 139–146.

28. Umamaheswari, R., Ramach, S. and Nobi, E. P., Mapping the extend of seagrass meadows of Gulf of Mannar Biosphere Reserve, India using IRS ID satellite imagery. *Int. J. Biodiver. Conserv.*, 2009, **1**(5), 187–193.
29. Das, H. S., Status of seagrass habitats of the Andaman and Nicobar coast. Technical Report 4, Salim Ali Centre for Ornithology and Natural History (SACON), Coimbatore, India, 1996.
30. Thangaradjou, T., Sivakumar, K., Nobi, E. P. and Dilipan, E., Distribution of seagrasses along the Andaman and Nicobar Islands: a post tsunami survey. In *Recent Trends in Biodiversity of Andaman and Nicobar Islands*, Zoological Survey of India, Kolkata, 2010, Chapter 11, pp. 157–160.
31. Savurirajan, M., Equbal, J., Lakra, R. K., Satyam, K. and Thiruchitrambalam, G., Species diversity and distribution of seagrasses from the South Andaman, Andaman and Nicobar Islands, India. *Bot. Mar.*, 2018, **61**(3), 225–234.
32. Paulose, N. E., Dilipan, E. and Thangaradjou, T., Integrating Indian remote sensing multi-spectral satellite and field data to estimate seagrass cover change in the Andaman and Nicobar Islands, India. *Ocean Sci. J.*, 2013, **48**(2), 173–181.
33. Dsouza, E. and Patankar, V., First underwater sighting and preliminary behavioural observations of Dugongs (*Dugong dugon*) in the wild from Indian waters, Andaman Islands. *J. Threatened Taxa*, 2009, **1**(1), 49–53.
34. NITI Aayog Report, Transforming the Islands through Creativity and Innovation, 2019.
35. Island wise – Area and Population, Census 2011.
36. Sen2Cor Configuration and User Manual, Ref. S2-PDGS-MPC-L2A-SUM- V2.5.5 (European Space Agency), 2018.
37. Qasim, S. Z. and Ansari, Z. A., Food components of the Andaman Sea, *Indian J. Marine Sci*., 1981, **10**(3), 276–279.
38. D'Souza, E., Patankar, V., Arthur, R., Marbà, N. and Alcoverro, T., Seagrass herbivory levels sustain site-fidelity in a remnant dugong population. *PLoS ONE*, 2015, **10**(10), e0141224.
39. Waycott, M., Duarte, C. M., Carruthers, T. J., Orth, R. J., Dennison, W. C., Olyarnik, S. and Kendrick, G. A., Accelerating loss of seagrasses across the globe threatens coastal ecosystems. *Proc. Natl. Acad. Sci.*, 2009, **106**(30), 12377–12381.
40. Short, F. T., Polidoro, B., Livingstone, S. R., Carpenter, K. E., Bandeira, S., Bujang, J. S. and Erftemeijer, P. L., Extinction risk assessment of the world's seagrass species. *Biol. Conserv.*, 2011, **144**(7), 1961–1971.
41. Sridhar, R., Thangaradjou, T., Kannan, L. and Astalakshmi, S., Assessment of coastal bio-resources of the Palk Bay, India, using IRS-LISS-III data. *J. Indian Soc. Remote Sensing*, 2010, **38**(3), 565–575.

ACKNOWLEDGEMENTS. We thank CAMPA Authority of the Ministry of Environment, Forest and Climate Change, Government of India for funding this study. We would like to thank CSSTEAP, Director (CSSTEAP) and Director (IIRS) for their support and facilities. We thank the State Forest Department of Andaman and Nicobar Islands and Prasad Gaidhani for support during field work. We are grateful to Director, Wildlife Institute of India and Director, Indian Institute of Remote Sensing for their constant encouragement.

Received 9 September 2019; revised accepted 3 January 2020

doi: 10.18520/cs/v118/i8/1275-1282

Development of wind speed retrieval model using RISAT-1 SAR cross-polarized observations

Jagdish Prajapati[1,2,*], Abhisek Chakraborty[1], Bipasha Paul Shukla[1] and Raj Kumar[1]

[1]Earth, Ocean, Atmosphere, Planetary Sciences and Applications Area, Space Applications Centre, Indian Space Research Organisation, Ahmedabad 380 015, India
[2]Department of Mathematics, Gujarat University, Ahmedabad 380 009, India

In this study, a method for retrieving ocean surface wind speed using C-band cross-polarization SAR observations has been outlined. A linear least square technique has been used to develop a Geophysical Model Function (GMF), C2P. The GMF was derived using NRCS observations from RISAT-1 and wind-speed observations from ASCAT. The correlation between observed and simulated NRCS values obtained from C2P was 0.66, with a negative bias of 0.01 dB and the corresponding root mean square difference of 1.13 dB. Subsequently, the developed GMF was tested with 774 RISAT-1 MRS datasets to retrieve wind speed along the Indian coast and also of the tropical cyclone 'Megh'. The measured intensity and radius of maximum wind speed were 30 m s^{-1} and 16.65 km respectively. Subsequently, the retrieved wind speed was validated with ASCAT wind-speed observations. The statistical comparison of RISAT-1 and ASCAT observed wind speed showed negative biases of 0.90 and 0.34 m s^{-1} with the corresponding RMSD of 2.11 and 1.77 m s^{-1} respectively, for CMOD5.N and C2P. The developed GMF C2P showed 16% more accuracy than that of CMOD5.N.

Keywords: Cross-polarization, geophysical model function, ocean surface, wind speed retrieval.

OCEAN surface winds are highly important for numerical weather and ocean state forecasting, study of oceanic transportation and processes occurring at the air–sea interface. For the last four decades, ocean surface vector winds at synoptic scales are operationally being retrieved from spaceborne scatterometers. Such observations of ocean surface winds are assimilated in numerical models for improving operational forecasts at moderate resolution. Scatterometer-based observations are available with coarser spatial resolution in the range 12–50 km with wider data gaps in the coastal regions. However, wind intensity of cyclones computed using Ku-band scatterometer data tends to underestimate the actual scenario. Therefore, in extreme conditions like cyclones, backscattered power received by microwave scatterometers mainly

*For correspondence. (e-mail: jagdish.aug1991@gmail.com)